# Table S1.
# Common insertion sites from the *Nras*mutant AMLs

| GENE | AML | LOCATION | DISTANCE | DIRECTION | ADDRESS | FREQUENCY |
|---|---|---|---|---|---|---|
| Evi 1 | 8021 | 5 prime | 8.74 kb | inv | 30197481 | 50 |
| | 8052 | 5 prime | 15.34 kb | same | 30204077 | 38 |
| | 8059 | 5 prime | 15.31 kb | same | 30204050 | 13 |
| | 8056 | 5 prime | 15.59 kb | same | 30204331 | 6 |
| | 8064 | 5 prime | 13.89 kb | inv | 30202625 | 10 |
| Sox 4 | 8057 | 3 prime | 116.60 kb | same | 28841593 | 53 |
| | 8057 | 3 prime | 179.73 kb | inv | 28778467 | 12 |
| | 8064 | 3 prime | 0.24 kb | inv | 28957957 | 1 |
| Myb | 8021 | intron 3 | disrupt CDS | inv | 20842957 | 1 |
| | 8064 | intron 3 | disrupt CDS | inv | 20843528 | 1 |
| Ap3b1 | 8021 | intron 7 | disrupt CDS | same | 95527768 | 1 |
| | 8052 | 5 prime | 31.09 kb | inv | 95428636 | 2 |
| Ctdp1 | 8052 | intron 10 | disrupt CDS | same | 80599081 | 2 |
| | 8064 | 5 prime | 55.77 kb | inv | 80687498 | 1 |

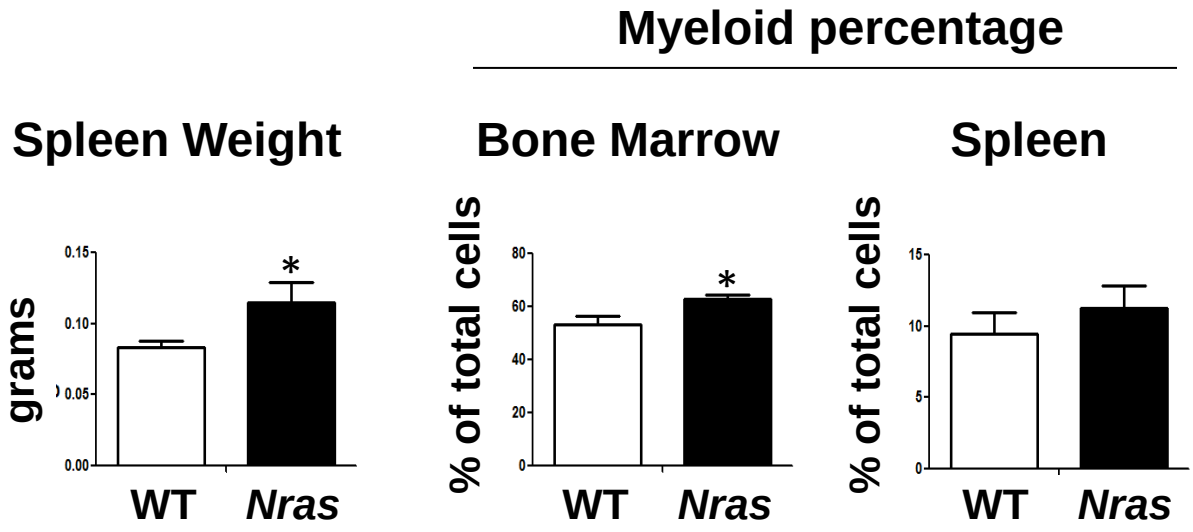


**Figure S1. Myeloid infiltration in *Nras*$^{G12D}$ mutant bone marrow and spleen 2 weeks after pIpC injection.** Asterisks indicate significant differences between these groups ($p < 0.05$).

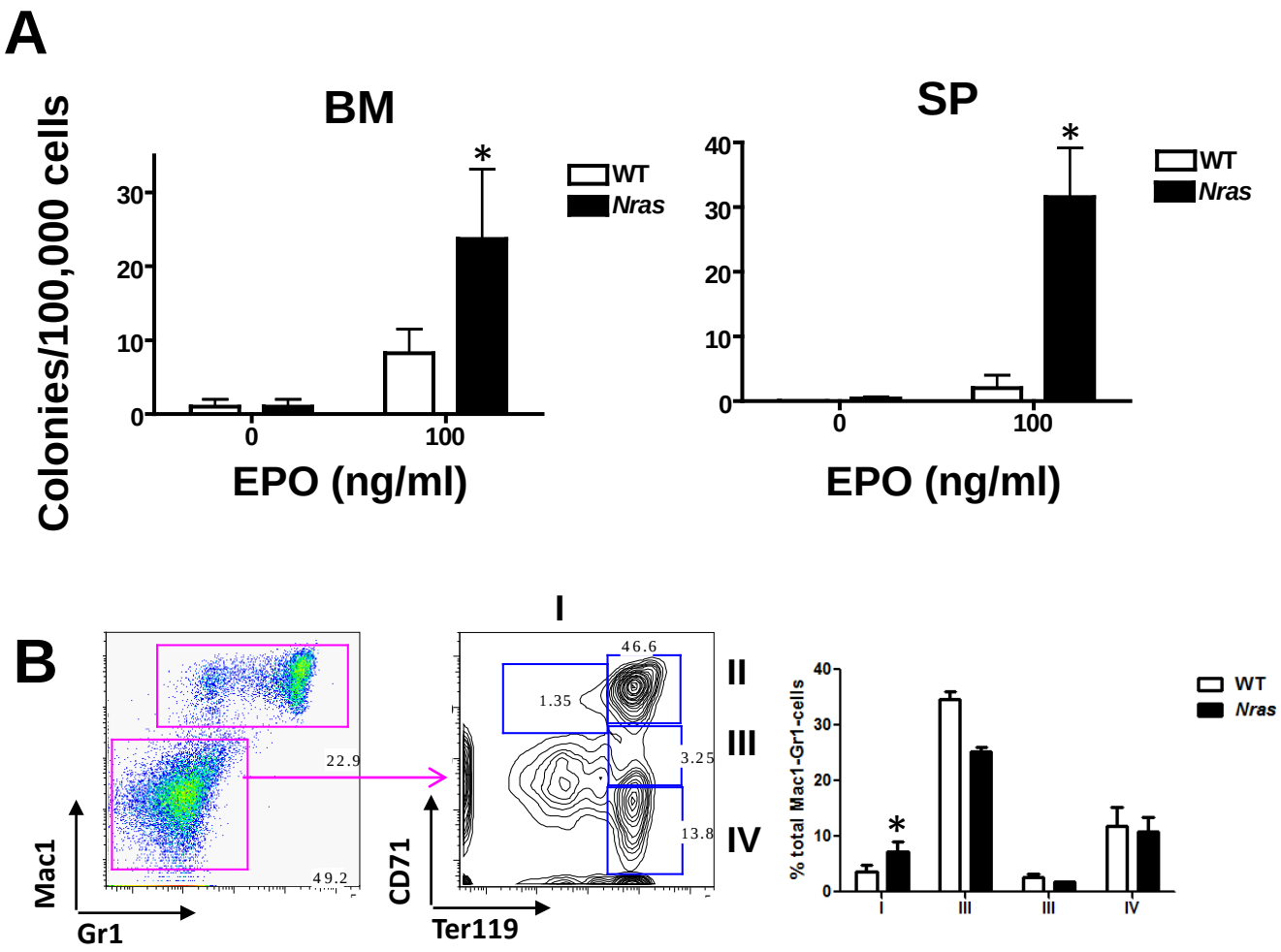


**Figure S2. Ineffective erythropoiesis in *Mx1-Cre, Nras$^{G12D}$* mice.** Hematopoietic tissues from *Mx1-Cre, Nras$^{G12D}$* mice that appeared well at 6 months of age were analyzed in parallel with specimens from littermate control animals. (A) BFU-E colony growth from WT and *Nras* mutant bone marrow cells (BM) and splenocytes (SP) were enumerated in methylcelllulose medium with and without a saturating concentration of erythropoietin (EPO; 100 ng/ml). (B) Erythroid differentiation was analyzed by flow cytometry using the cell surface markers CD71 and Ter119. The cells were first stained with myeloid markers Mac1 and Gr1 to exclude myeloid lineage cells. As erythroid cells differentiate, they migrate from region I, to II and III, and eventually to IV, which represents mature cells. The percentages of WT and *Nras* mutant cells in each region were shown at the bottom of panel B. Asterisks indicate significant differences between these groups ($p < 0.05$).

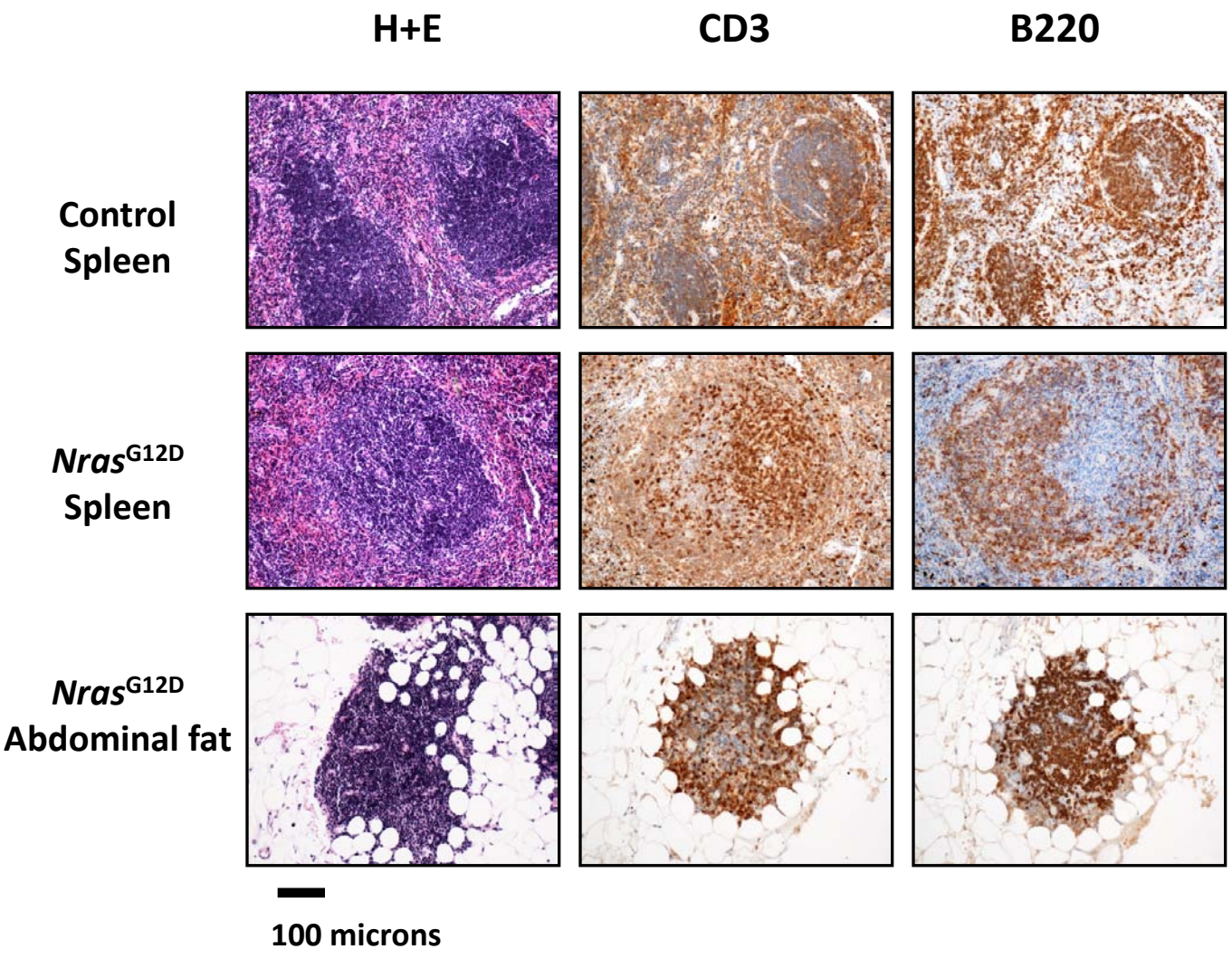


**Figure S3. *Nras*$^{G12D}$ expression induces polyclonal lymphoid proliferation.** Histopathology (H & E, left panel) of WT and *Mx1-Cre, Nras*$^{G12D}$ animals showed expansion of white pulps of spleen and extranodal infiltration of lymphocytes in the *Nras* mutants. Immunohistochemistry of tissue sections with B220 and CD3 (middle and right panels) antibodies showed mixed B and T cells in the infiltrated organs.

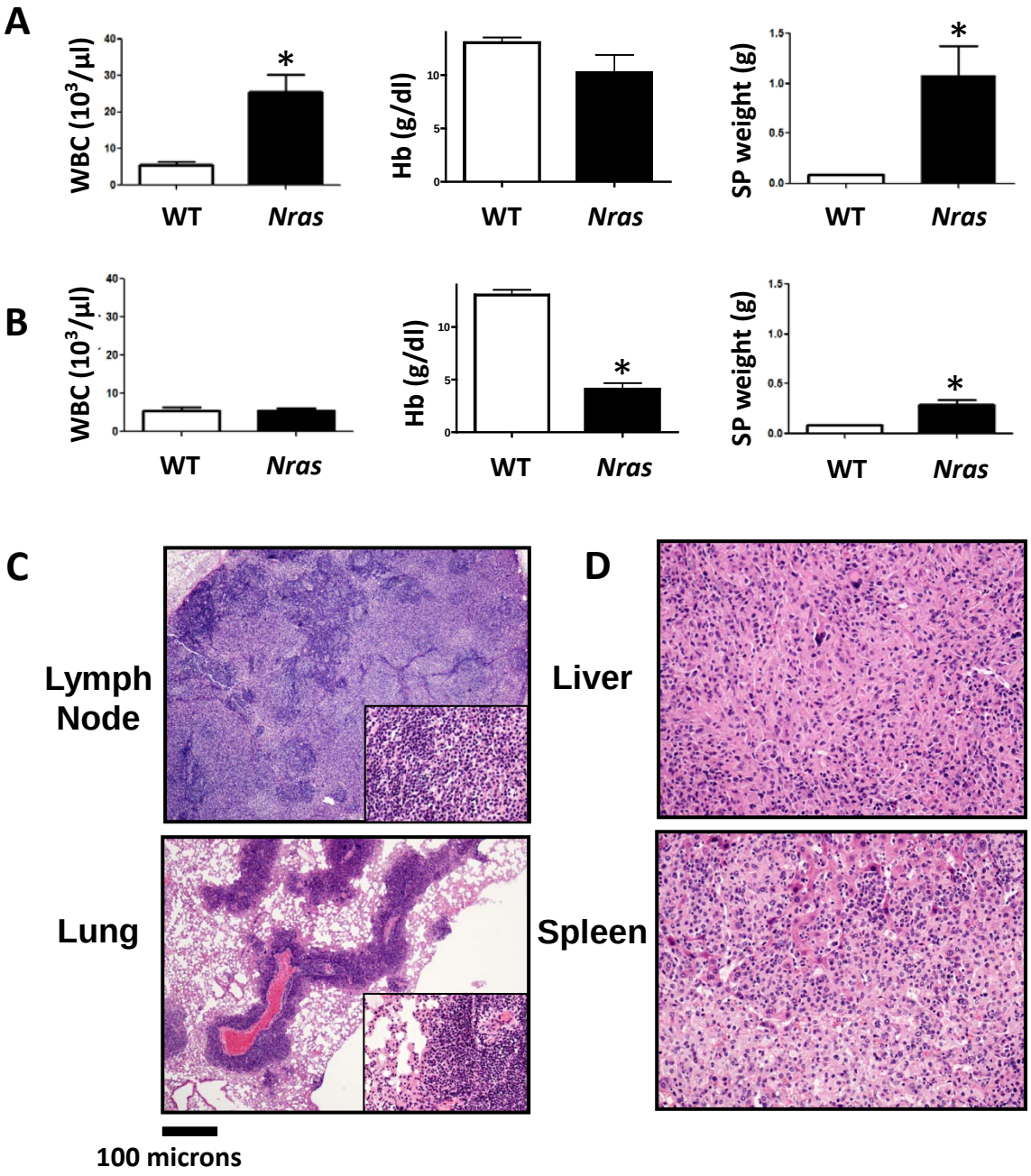


**Figure S4. Moribund *Mx1-Cre, Nras$^{G12D}$* mice develop a spectrum of hematopoietic malignancies.** (A) Mean white blood cell counts (WBC), hemoglobin concentrations (Hb), and spleen (SP) weight in *Mx1-Cre, Nras$^{G12D}$* mice that died with MPD (n=5) and WT littermates (n=5). (B) WBC, Hb, and spleen (SP) weight in *Mx1-Cre, Nras$^{G12D}$* mice that were classified as dying from MDS (n=4) and WT littermates (n=5). (C) Lymphoid infiltration of lymph node and lung in *Mx1-Cre, Nras$^{G12D}$* mice that died with mixed MPD and lymphoproliferation. (D) Liver and spleen sections from *Mx1-Cre, Nras$^{G12D}$* mice that died from histiocytic sarcoma. *Mx1-Cre, Nras$^{G12D}$* mice and wild type littermates on a C57BL6 x 129Sv F1 strain background were used in these analyses. Panels C and D are histograms at the 40X magnification. Asterisks indicate significant differences between these groups ($p < 0.05$).

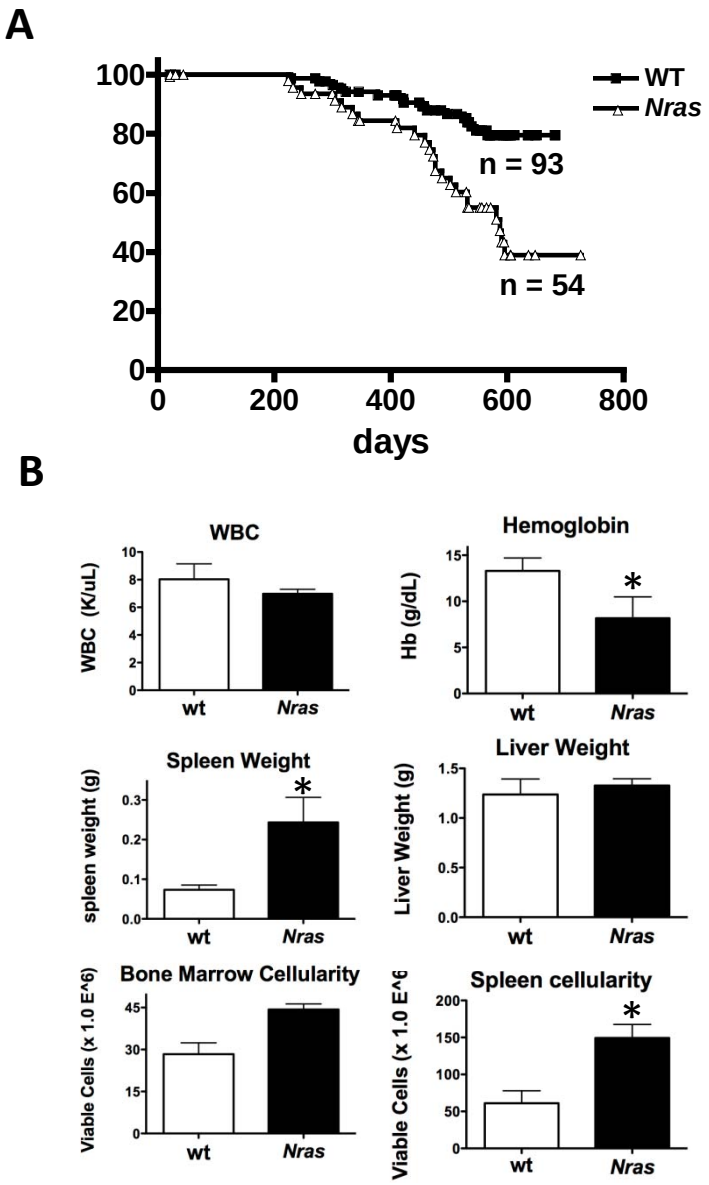


**Figure S5. Phenotype of the *Mx1-Cre, Nras$^{G12D}$* mice on the C57Bl/6 strain background.** (A) Kaplan-Meier survival curve shows reduced survival of *Mx1-Cre, Nras$^{G12D}$* mice compared to control littermates (p= 0.0032). (B) White blood cell (WBC), hemoglobin (Hb), spleen weight, liver weight, and bone marrow and liver cellularity in WT (n = 3 ) and *Nras* mutant (n = 6) mice that appeared well at 6 months of age. Asterisks indicate significant differences between these groups ($p < 0.05$).

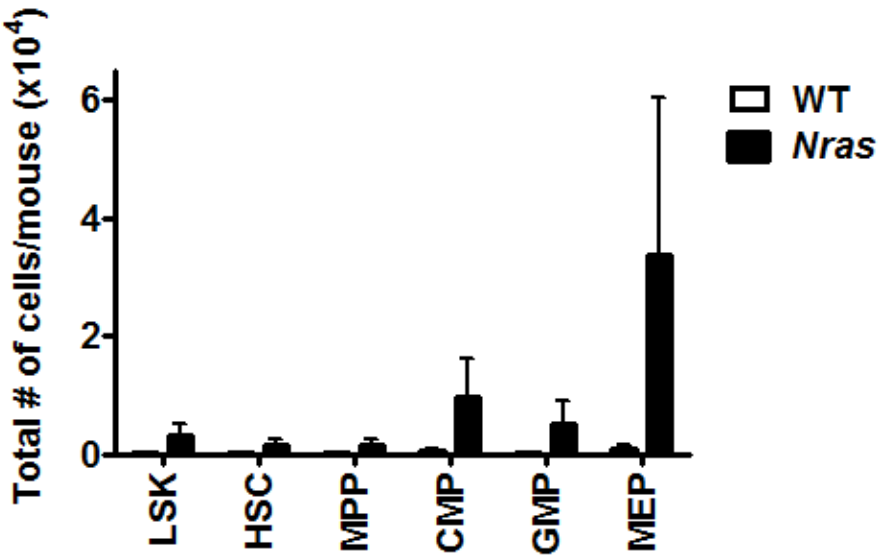


**Figure S6. HSC and myeloid progenitor populations were increased in the *Nras* mutant spleen.** Summary of stem cell and progenitor cell populations analyzed as previously described (Passegué E, et al, J Exp Med. 202(11):1599-611).

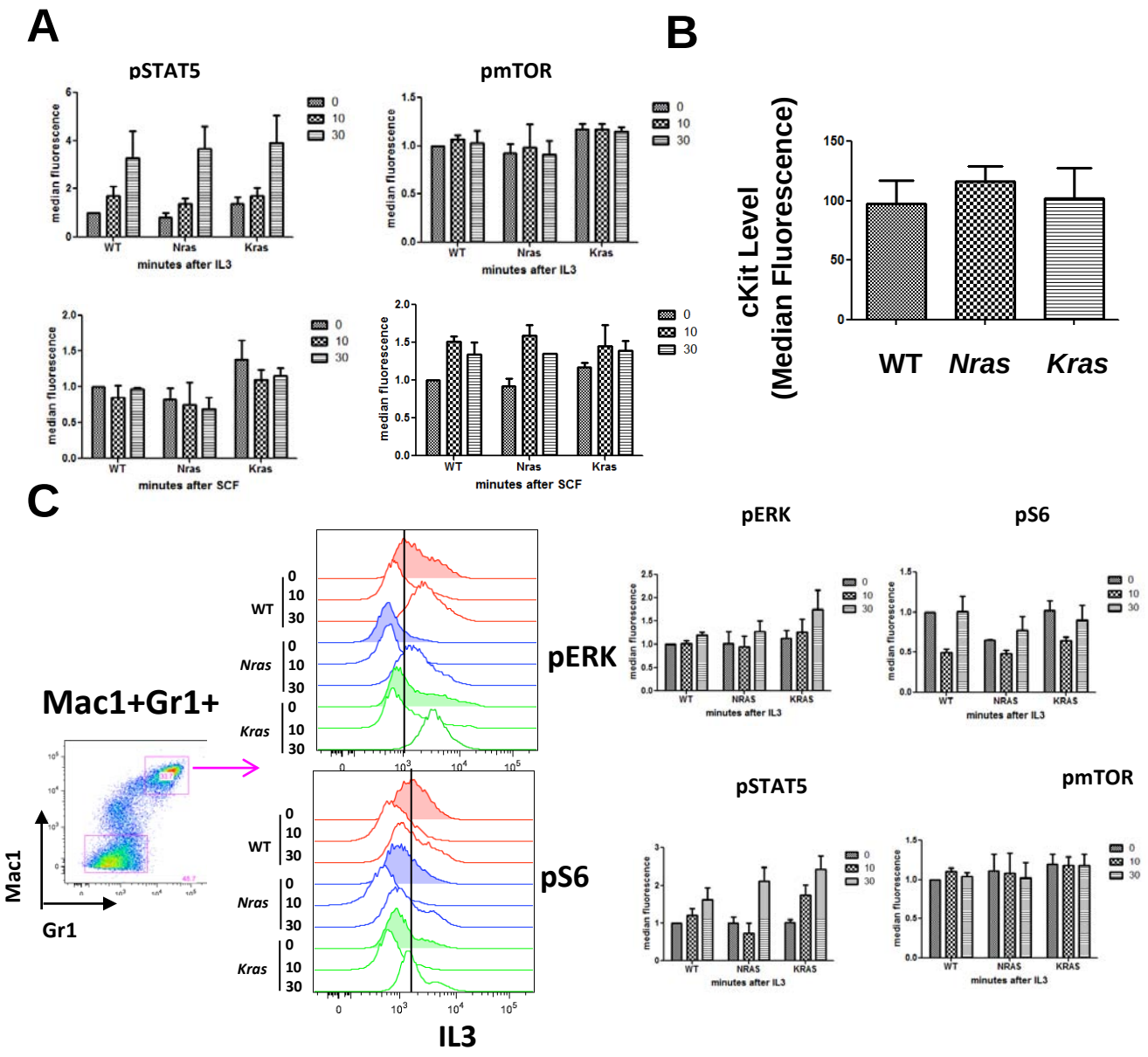


**Figure S7. Signaling in WT, *Nras* and *Kras* mutant bone marrow cells.**(A) phospho-FACS of pSTAT5 and pmTOR in Mac1-Gr1-cKit+ cells before and after incubation with IL-3 (50ng/ml) or SCF (100ng/ml). (B) levels of cKit protein measured by pFACS in WT, *Nras* and *Kras* mutant cells. (C) phospho – ERK, S6, STAT5 and mTOR iin Mac1+Gr1+ bone marrow cells before and after stimulation with IL-3 (50ng/ml).

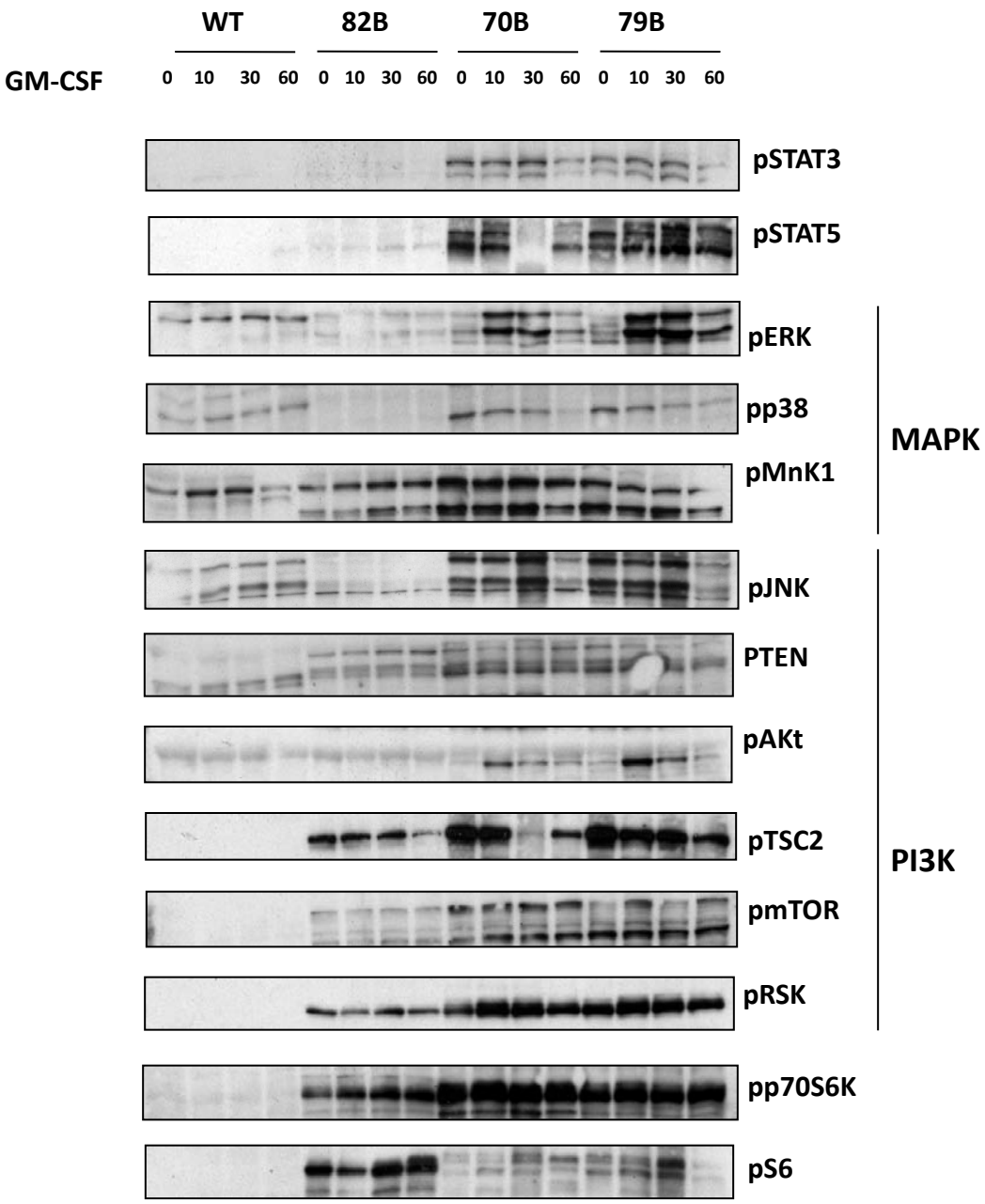


**Figure S8. Western analysis of signaling proteins of Ras downstream effectors.** Bone marrow cells were harvested from wild type (WT) and *Nras* mutant AMLs (82B, 70B, 79B). Cells were starved for 2 hours and then stimulated for 10, 30 and 60 minutes with GM-CSF 10ng/ml.